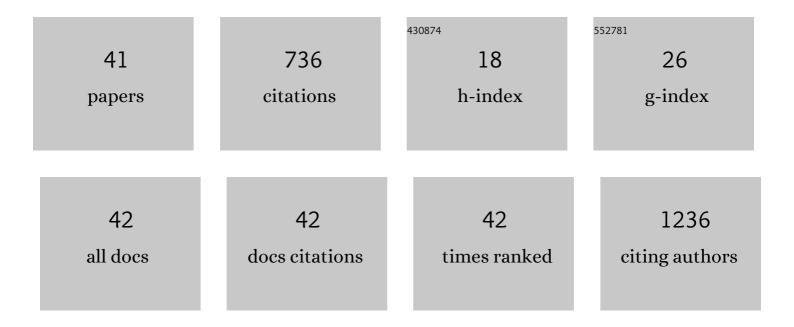
## Alessandro Gambardella

List of Publications by Year in descending order

Source: https://exaly.com/author-pdf/1157441/publications.pdf Version: 2024-02-01



#	Article	IF	CITATIONS
1	Isolated Mn12Single-Molecule Magnets Grafted on Gold Surfaces via Electrostatic Interactions. Inorganic Chemistry, 2005, 44, 7693-7695.	4.0	72
2	Strontium doped calcium phosphate coatings on poly(etheretherketone) (PEEK) by pulsed electron deposition. Surface and Coatings Technology, 2017, 319, 191-199.	4.8	38
3	Isolated Heterometallic Cr7Ni Rings Grafted on Au(111) Surface. Inorganic Chemistry, 2007, 46, 4937-4943.	4.0	36
4	Tribological characterization of zirconia coatings deposited on Ti6Al4V components for orthopedic applications. Materials Science and Engineering C, 2016, 62, 643-655.	7.3	35
5	Nano-Based Biomaterials as Drug Delivery Systems Against Osteoporosis: A Systematic Review of Preclinical and Clinical Evidence. Nanomaterials, 2021, 11, 530.	4.1	33
6	Fabrication and characterization of biomimetic hydroxyapatite thin films for bone implants by direct ablation of a biogenic source. Materials Science and Engineering C, 2019, 99, 853-862.	7.3	32
7	Composite Scaffolds for Bone Tissue Regeneration Based on PCL and Mg-Containing Bioactive Glasses. Biology, 2021, 10, 398.	2.8	30
8	Conditions for the growth of smooth La0.7Sr0.3MnO3 thin films by pulsed electron ablation. Thin Solid Films, 2013, 534, 83-89.	1.8	28
9	A comparative study of the growth dynamics of zirconia thin films deposited by ionized jet deposition onto different substrates. Surface and Coatings Technology, 2018, 337, 306-312.	4.8	27
10	Tough and adhesive nanostructured calcium phosphate thin films deposited by the pulsed plasma deposition method. RSC Advances, 2015, 5, 78561-78571.	3.6	26
11	Magnetic hydroxyapatite coatings as a new tool in medicine: A scanning probe investigation. Materials Science and Engineering C, 2016, 62, 444-449.	7.3	26
12	Pulsed Electron Deposition of nanostructured bioactive glass coatings for biomedical applications. Ceramics International, 2017, 43, 15862-15867.	4.8	26
13	Electronic and Magnetic Properties of Mn12 Molecular Magnets on Sulfonate and Carboxylic Acid Prefunctionalized Gold Surfaces. Journal of Physical Chemistry C, 2012, 116, 14936-14942.	3.1	24
14	Polaron framework to account for transport properties in metallic epitaxial manganite films. Physical Review B, 2014, 89, .	3.2	24
15	Surface morphology, tribological properties and in vitro biocompatibility of nanostructured zirconia thin films. Journal of Materials Science: Materials in Medicine, 2016, 27, 96.	3.6	24
16	Tunnel conductivity switching in a single nanoparticle-based nano floating gate memory. Scientific Reports, 2014, 4, 4196.	3.3	21
17	Nanostructured Ag thin films deposited by pulsed electron ablation. Applied Surface Science, 2019, 475, 917-925.	6.1	21
18	Multifunctional 3D-Printed Magnetic Polycaprolactone/Hydroxyapatite Scaffolds for Bone Tissue Engineering. Polymers, 2021, 13, 3825.	4.5	20

#	Article	IF	CITATIONS
19	Transport properties ofNd1.2Ba1.8Cu3OZultrathin films by field-effect doping. Physical Review B, 2004, 70, .	3.2	18
20	Plasma-assisted deposition of bone apatite-like thin films from natural apatite. Materials Letters, 2017, 199, 32-36.	2.6	18
21	Osteogenic Differentiation of hDPSCs on Biogenic Bone Apatite Thin Films. Stem Cells International, 2017, 2017, 1-10.	2.5	17
22	Self-assembling of Mn12 molecular nanomagnets on FIB-patterned Au dot matrix. Surface Science, 2007, 601, 2618-2622.	1.9	16
23	CERAMIC THIN FILMS REALIZED BY MEANS OF PULSED PLASMA DEPOSITION TECHNIQUE: APPLICATIONS FOR ORTHOPEDICS. Journal of Mechanics in Medicine and Biology, 2015, 15, 1540002.	0.7	14
24	Optimizing thickness of ceramic coatings on plastic components for orthopedic applications: A finite element analysis. Materials Science and Engineering C, 2016, 58, 381-388.	7.3	13
25	Chemical states and ferromagnetism in heavily Mn-substituted zinc oxide thin films. Journal of Applied Physics, 2014, 115, .	2.5	12
26	Nanoindentation: An advanced procedure to investigate osteochondral engineered tissues. Journal of the Mechanical Behavior of Biomedical Materials, 2019, 96, 79-87.	3.1	12
27	Electronic phase separation near the superconductor-insulator transition of <mml:math display="inline" xmlns:mml="http://www.w3.org/1998/Math/MathML"> <mml:mrow> <mm< td=""><td>&gt; <sup>3</sup>ifiml:mi</td><td>ı&gt;¹P</td></mm<></mml:mrow></mml:mrow></mml:mrow></mml:mrow></mml:mrow></mml:mrow></mml:mrow></mml:mrow></mml:mrow></mml:mrow></mml:mrow></mml:mrow></mml:mrow></mml:mrow></mml:mrow></mml:mrow></mml:mrow></mml:mrow></mml:mrow></mml:mrow></mml:mrow></mml:mrow></mml:mrow></mml:mrow></mml:mrow></mml:mrow></mml:mrow></mml:mrow></mml:mrow></mml:mrow></mml:mrow></mml:mrow></mml:mrow></mml:mrow></mml:mrow></mml:mrow></mml:mrow></mml:mrow></mml:mrow></mml:mrow></mml:mrow></mml:mrow></mml:mrow></mml:mrow></mml:mrow></mml:mrow></mml:mrow></mml:mrow></mml:mrow></mml:mrow></mml:mrow></mml:mrow></mml:mrow></mml:mrow></mml:mrow></mml:mrow></mml:mrow></mml:mrow></mml:mrow></mml:mrow></mml:mrow></mml:mrow></mml:mrow></mml:mrow></mml:mrow></mml:mrow></mml:mrow></mml:mrow></mml:mrow></mml:mrow></mml:mrow></mml:mrow></mml:mrow></mml:mrow></mml:mrow></mml:mrow></mml:mrow></mml:mrow></mml:mrow></mml:mrow></mml:mrow></mml:mrow></mml:mrow></mml:mrow></mml:mrow></mml:mrow></mml:mrow></mml:mrow></mml:mrow></mml:mrow></mml:mrow></mml:mrow></mml:mrow></mml:mrow></mml:mrow></mml:mrow></mml:mrow></mml:mrow></mml:mrow></mml:mrow></mml:mrow></mml:mrow></mml:mrow></mml:mrow></mml:mrow></mml:mrow></mml:mrow></mml:mrow></mml:mrow></mml:mrow></mml:mrow></mml:mrow></mml:mrow></mml:mrow></mml:mrow></mml:mrow></mml:mrow></mml:mrow></mml:mrow></mml:mrow></mml:mrow></mml:mrow></mml:mrow></mml:mrow></mml:mrow></mml:mrow></mml:mrow></mml:mrow></mml:mrow></mml:mrow></mml:mrow></mml:mrow></mml:mrow></mml:mrow></mml:mrow></mml:mrow></mml:mrow></mml:mrow></mml:mrow></mml:mrow></mml:mrow></mml:mrow></mml:mrow></mml:mrow></mml:mrow></mml:mrow></mml:mrow></mml:mrow></mml:mrow></mml:mrow></mml:mrow></mml:mrow></mml:mrow></mml:mrow></mml:mrow></mml:mrow></mml:mrow></mml:mrow></mml:mrow></mml:mrow></mml:mrow></mml:mrow></mml:mrow></mml:mrow></mml:mrow></mml:mrow></mml:mrow></mml:mrow></mml:mrow></mml:mrow></mml:mrow></mml:mrow></mml:math>	> <sup>3</sup> ifiml:mi	ı>¹P
28	Surface Nanostructures in Manganite Films. Scientific Reports, 2014, 4, 5353.	3.3	10
29	Monitoring morphological and chemical properties during silver solid-state dewetting. Applied Surface Science, 2019, 498, 143890.	6.1	9
30	Electric field effect and superconducting–insulating transition in â€~123' cuprate superconductors. Superconductor Science and Technology, 2009, 22, 034010.	3.5	5
31	Effects of working gas pressure on zirconium dioxide thin film prepared by pulsed plasma deposition: roughness, wettability, friction and wear characteristics. Journal of the Mechanical Behavior of Biomedical Materials, 2017, 72, 200-208.	3.1	5
32	Determination of the Spatial Anisotropy of the Surface MicroStructures of Different Implant Materials: An Atomic Force Microscopy Study. Materials, 2021, 14, 4803.	2.9	5
33	Ceramic coatings for orthopaedic implants: preparation and characterization. Surface and Interface Analysis, 2016, 48, 616-620.	1.8	3
34	Roughness conformality during thin films deposition onto rough substrates: A quantitative study. Thin Solid Films, 2020, 709, 138258.	1.8	3
35	Assessing conformal thin film growth under nonstochastic deposition conditions: application of a phenomenological model of roughness replication to synthetic topographic images. Journal of Microscopy, 2020, 280, 270-279.	1.8	3
36	Impact of Surface Functionalization by Nanostructured Silver Thin Films on Thermoplastic Central Venous Catheters: Mechanical, Microscopical and Thermal Analyses. Coatings, 2020, 10, 1034.	2.6	3

#	Article	IF	CITATIONS
37	Comparison among superconducting models for β″-ET4[(H3O)Fe(C2O4)3]·C6H5Br single crystals by scanning tunnelling spectroscopy. Solid State Sciences, 2008, 10, 1773-1776.	3.2	2
38	Scanning tunnelling spectroscopy study of paramagnetic superconducting β′′-ET4[(H3O)Fe(C2O4)3]·C6H5Br crystals. Journal of Physics Condensed Matter, 2010, 22, 175701.	1.8	2
39	Seed layer technique for high quality epitaxial manganite films. AIP Advances, 2016, 6, 085109.	1.3	2
40	Ultrathin hydroxyapatite coating on pure magnesium substrate prepared by pulsed electron ablation technique. Materials and Corrosion - Werkstoffe Und Korrosion, 2020, 71, 1794-1801.	1.5	2
41	Electrostatic Modulation of Conductivity in <tex>\$rm Nd_1.2rm Ba_1.8rm Cu_3rm O_rm y\$</tex> Thin Films. IEEE Transactions on Applied Superconductivity, 2005, 15, 2946-2949.	1.7	1